Low-cost Polyurethane Coating as Dielectric Component in Digital Microfluidics

E. N. Abdul Latip[1, 2], L. Coudron[1], M. C. Tracey[1]*
[1]School of Physics, Engineering & Computer Science,
University of Hertfordshire,
College Lane, Hatfield, AL10 9AB, UK
[2]School of Mechanical Engineering, College of Engineering,
Universiti Teknologi MARA, 40450 Shah Alam, MALAYSIA
**elinadia@uitm.edu.my*

ABSTRACT

Digital microfluidics (DMF) as a platform for precise handling of liquid droplets is a powerful tool but the affordability of the device has been one of the hindrances to its wide implementation. This paper reports the development of DMF devices using low-cost materials and simple deposition techniques specifically for the device dielectric component. Three commercial polyurethane coatings were investigated for their feasibility as the dielectric layer. The electrowetting behaviour of these materials was investigated by evaluating the change in contact angle with applied voltage of a water droplet sitting on the dielectric samples prepared using easy deposition methods such as spraying and spin coating. Devices were then fabricated using these materials to evaluate their capability to actuate droplets. Five types of polyurethane dielectric sample exhibited contact angle reversibility with hysteresis ranging between 4° to 25° after 250 V_{DC} application. Droplet transportation back and forth across 8 electrodes at 180 V_{RMS} has been demonstrated in a device made of one of the polyurethane coatings using a spraying technique. This result implies the potential of using polyurethane for future development of low-cost and disposable DMF devices.

Keywords: *Digital Microfluidics; Polyurethane; Electrowetting-On-Dielectric*

ISSN 1823-5514, eISSN 2550-164X

https://doi.org/10.24191/jmeche.v20i1.21082

Received for review: 2022-06-30
Accepted for publication: 2022-12-20
Published: 2023-01-15

Introduction

Digital microfluidics (DMF) manipulates multiple individual droplets to move, mix, merge, and split on a surface using electrowetting-on-dielectric (EWOD) mechanism to perform specific functions such as sample preparation, DNA amplification and immunoassays [1]–[3] in a lab-on-a-chip platform. The volume of droplet required in a DMF device is in the microliter range, resulting in reduced consumption of sample and reagents and fast results. EWOD controls droplets by electrostatic energy, allowing for fully-automated devices with simple design to be realised [4]-[5]. Another advantage of an EWOD-based DMF device is its open architecture where no physical features such as micro-channels, pumps or valves are necessary, making it a versatile tool that can be reconfigured to perform more than one function [6]. An EWOD device typically consists of a base plate composed of a substrate patterned with control electrodes. These electrodes are buried underneath a layer of dielectric material which generates electric fields when a voltage is applied across the dielectric layer [1]–[7].

The dielectric layer sustains the capacitance or the electrostatic energy that drives the droplet actuation by preventing electron transfer from the electrodes to the droplet. The change in contact angle of a water droplet sitting on an electrode coated with a dielectric layer when a voltage is applied is regulated by the following Young-Lippmann equation:

$$cos\,\theta_v = cos\,\theta + \frac{1}{2\,\gamma_{lg}} cV^2 \qquad (1)$$

where θ_v is CA at applied voltage, θ is initial CA, γ_{lg} is liquid-gas surface tension, and V is the applied voltage. The capacitance per unit area, c is equivalent to $\frac{\varepsilon_o \varepsilon_r}{d}$ where ε_o is the vacuum permittivity, ε_r is the dielectric constant, and d is the dielectric thickness.

Ideally, the dielectric material should have a high dielectric constant which will result in a higher electrostatic energy to actuate droplets more efficiently. To ensure a reliable electrowetting performance, it is also desirable for the dielectric material to have a high CA reversibility, i.e. low hysteresis after an electrowetting cycle, indicating no charges are trapped in the layer after removal of voltage [8]-[9].

While there are numerous reports of DMF devices in the academic literature, they have not been widely demonstrated as real-world point-of-care diagnostic platforms due to the high fabrication cost [5], [10]-[11]. For the device dielectric component, commonly used materials such as Parylene-C and Teflon™ AF are expensive while others, for example, silicon dioxide and aluminium oxide, require clean-room facilities and elaborate processes [8], [10]-[11]. Dielectric materials with superior dielectric constant such as

aluminium oxide (9.5) [12] and tantalum pentoxide (20-25) [13]-[14] possess the same challenge of requiring deposition techniques that are expensive and time consuming.

There were studies experimented with low-cost products such as Saran™ wrap [15] and parafilm [16] applied using simple deposition methods but the robustness and reliability of these materials have not been well-investigated and proven yet. Some studies attempt to overcome this by using low-cost material such as SU-8 [17]-[18] and PDMS [19]-[20]. These materials however pose another challenge which is the formation of pinholes in the layer [11]. Other unconventional materials for EWOD dielectric component that have been demonstrated are: ion gel [11], PMMA/fluoropolymer bilayer [21] and cyanoethyl pullulan [22]. All these alternative materials employed easy deposition techniques such as spin coating and roll coating. Meanwhile, Yamamoto et al. [23] replaced the solid dielectric layer by infusing the electrodes with silicone oil which acted as liquid dielectric.

This paper aims to explore the potential of readily available consumer products as the alternative to conventional dielectric materials. One of the products that can be utilised is polyurethane (PU) coating, typically used as a protection layer on various types of surfaces. Three types of PU coatings were investigated for their feasibility as dielectric component. The contact angle (CA) evolution of a deionised (DI) water droplet sitting on the dielectric surface as a function of applied voltage was measured. If the CA of the water droplet was found to be reversible after voltage application, further investigation was conducted by employing the material in the EWOD plate fabrication to evaluate whether droplet transportation could be established.

Materials and Methods

Dielectric sample preparation

The samples for CA measurement, structure shown in Figure 1, consist of a silicon wafer substrate (p-type, <100>, 1-10 Ω·cm, Pi-Kem Ltd), a dielectric layer, and a hydrophobic coating (Cytop®, Asahi Glass Co., Ltd.). Three types of products were investigated: Blackfriar Polyurethane Varnish (BF), Rust-Oleum® Polyurethane Finish (RO-PU), and Rust-Oleum® Crystal Clear (RO-CC). The materials are supplied in liquid form inside aerosol cans except for BF which is a varnish in a metal container. The deposition methods used for each material are summarised in Table 1.

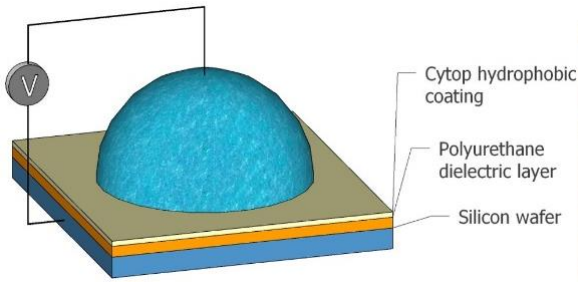

Figure 1: The dielectric sample's structure

Table 1: Deposition methods for dielectric materials

Dielectric material	Deposition method	Number of layers	Curing time and temperature
Blackfriar PU Varnish (BF)	Squeegee	1 and 2	24 hours, ambient temperature
Rust-Oleum® PU Finish (RO-PU)	Spraying	1 and 2	24 hours, ambient temperature
	Spin coating	1	1 hour, 100 °C
Rust-Oleum® Crystal Clear (RO-CC)	Spraying	1 and 2	24 hours, ambient temperature
	Spin coating	1	1 hour, 100 °C

For the two-layer samples, a second layer was applied after 2 hours of drying for the BF samples and after two minutes for the spray-coated samples (both RO-PU and RO-CC). Spin coating (LabSpin6, SUSS MicroTec) of the materials was performed at 1500 rpm for 30 s. The hydrophobic layer was spin-coated on top of the dielectric and cured for 30 minutes at 140 °C. The dielectric thickness was evaluated using a surface profilometer (AlphaStep® D-500, KLA Tencor).

Contact angle measurements

The CA measurements were performed using Theta Lite tensiometer (Biolin Scientific). A positive voltage was applied via a platinum wire to a DI water droplet (20 µl) sitting on the sample (set-up in Figure 2). The voltage was varied between 0 V and 250 V using a DC power supply (Digimess) and the CA value was identified at three levels: the initial 0 V, the maximum voltage at 250 V, and again at 0 V after voltage application. The voltage was increased to 250 V in approximately 20 seconds and left at the maximum level for about 10 seconds before returning to 0 V. The same steps were repeated with a lower maximum voltage, 150 V.

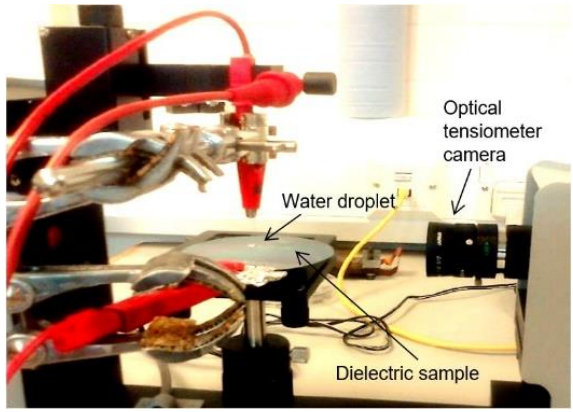

Figure 2: The CA measurement set-up

EWOD plates fabrication and droplet transportation

For each dielectric surface that demonstrated CA reversibility, two actuation plates were prepared using an identical deposition method as described previously. The EWOD plates design (Figure 3a and 3b) consisted of three rows of 16 square electrodes, 1.7 mm in nominal size with 200 µm nominal inter-electrode spacing. The parallel-plate configuration (Figure 3c) was employed with ITO-coated glass slide (Diamond Coatings) as the cover plate. The electrodes were made of PEDOT:PSS ink (Sigma Aldrich) patterned on a hydrophilic polyethylene terephthalate (PET) substrate using inkjet printing technique (Fujifilm Dimatix DMP-2850). The set-up and drive electronics for droplet actuation were similar to the one previously reported in [24]-[25].

Results and Discussion

Contact angle measurements

Figure 4 and Table 2 show the contact angle response of DI water droplet on different types of dielectric samples with applied voltage. Five types of surfaces have shown CA reversibility after 250 V voltage application, with thickness ranging from 9 to 71 µm. The spray-coated RO-PU and RO-CC samples exhibited reversibility on both one-layer and two-layer samples. The two-layer BF and one-layer spray-coated RO-CC demonstrated good reversibility with low hysteresis, 4° and 6° respectively with a wide range of CA modulation, both more than 40°. These results are comparable to 3.2 µm thickness Parylene-C employing the same Cytop® hydrophobic surface [13]. As predicted, the thicker the insulating layer, the narrower the CA modulation for any types of samples. Both of the two-layer spray-coated RO-PU and RO-

CC exhibited small CA change when 150 V was applied, requiring a higher voltage to induce larger CA change.

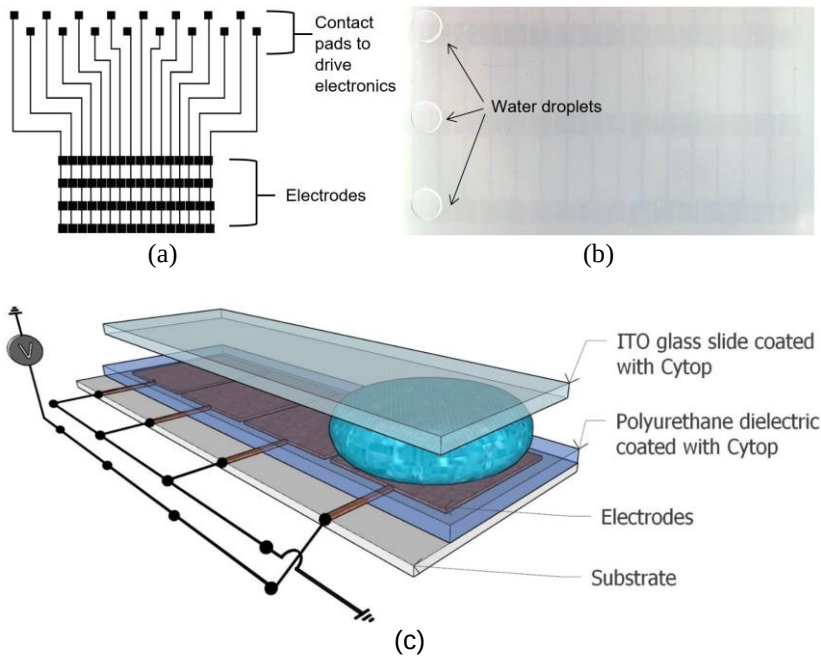

Figure 3: a) The design of the inkjet-printed EWOD plate, b) water droplets in the inkjet-printed device, and c) the parallel-plate configuration

As discussed previously, the Young-Lippmann equation governs the contact angle evolution with applied voltage and is given by equation 1 where the capacitance per unit area, c is equivalent to $\frac{\varepsilon_o \varepsilon_r}{d}$. The electrowetting number, $\frac{\varepsilon_o \varepsilon_r}{2\,\gamma_{lg} d}\,V^2$ at 150 V was calculated for all the reversible surfaces. This dimensionless number measures the electrostatic energy strength compared to the surface tension. Based on the calculated values, two-layer RO-PU is the least efficient at 150 V with the lowest electrowetting number (0.08) followed by two-layer RO-CC (0.09). The two-layer BF surface has the highest number (0.49), while one-layer RO-PU and one-layer RO-CC numbers are 0.39 and 0.38 respectively.

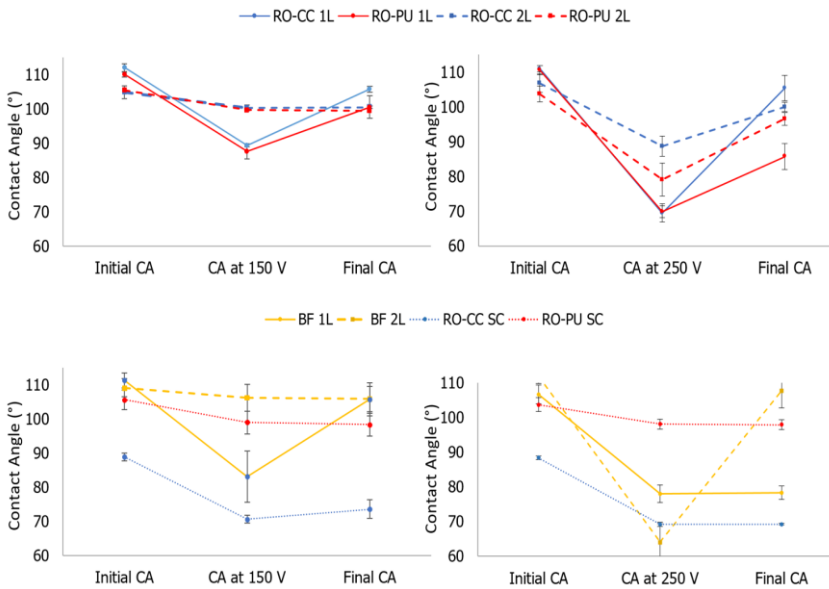

Figure 4: The CA response of the RO-CC (blue), RO-PU (red), and BF (yellow) materials. The solid lines denote the one-layer while the dashed lines denote the two-layer samples. The dotted lines represent the spin-coated samples

The one-layer BF and both spin-coated RO-CC and RO-PU were irreversible; it is suspected that formation of pinholes during dielectric deposition caused the failure. Bubbles generation can be observed (Figure 5) in the droplet due to electrolysis during the electrowetting cycle. In Figure 5a, bubbles began to form when voltage was increased, and more were generated in Figure 5b at higher voltage. Notice that the droplet CA has decreased in Figure 5b compared to in Figure 5a and it remained at the same value after removal of voltage application, demonstrating its irreversibility. All of the irreversible surfaces have thicknesses below 5 µm, indicating that more than one layer is required to produce a higher thickness to prevent pinholes formation and dielectric breakdown. However, it should be noted that if the thickness is too high it will affect the droplet actuation performance by increasing the operating voltage requirement [26]-[27].

Table 2: Electrowetting hysteresis, thickness, and electrowetting number of the dielectric samples

Dielectric material	No. of layer & deposition method	Hysteresis (°)	Electrowetting number at 150 V	Average thickness (µm)
Blackfriar PU Varnish (BF)	1-layer squeegee	Irreversible	-	0.5 ± 0.2
	2-layer squeegee	4 ± 5	0.49	9 ± 1
Rust-Oleum® PU Finish (RO-PU)	1-layer spray-coated	6 ± 4	0.38	26 ± 4
	2-layer spray-coated	7 ± 2	0.09	56 ± 7
	1-layer spin-coated	Irreversible	-	4.6 ± 0.3
Rust-Oleum® Crystal Clear (RO-CC)	1-layer spray-coated	25 ± 3	0.39	40 ± 10
	2-layer spray-coated	7.1 ± 0.8	0.08	71 ± 3
	1-layer spin-coated	Irreversible	-	1.83 ± 0.03

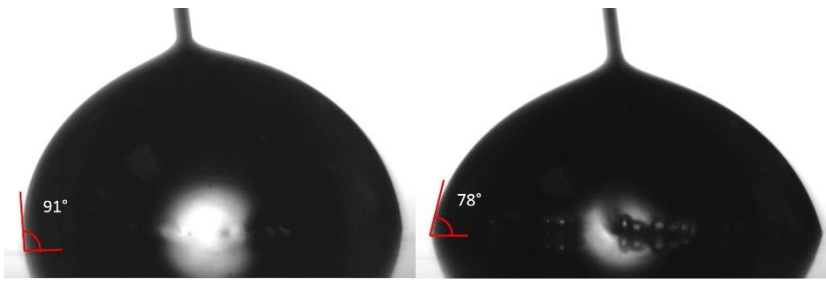

(a) (b)

Figure 5: Progressive bubbles development due to electrolysis in 20 µl water droplet sitting on one-layer BF sample; (a) bubbles formation at lower voltage, and (b) at higher voltage

The CA measurement for the one-layer RO-PU surface, which has the best actuation performance (discussed in the next section), during five successive cycles is presented in Figure 6. The CA at 0 V decreased after the completion of each cycle and reduced to 77° after the fifth cycle. The CA modulation also decreased as the repetition progressed with only about 7°

change induced during the 5th cycle. The CA at 250 V for each cycle were fairly constant, ranging between 68° to 71°.

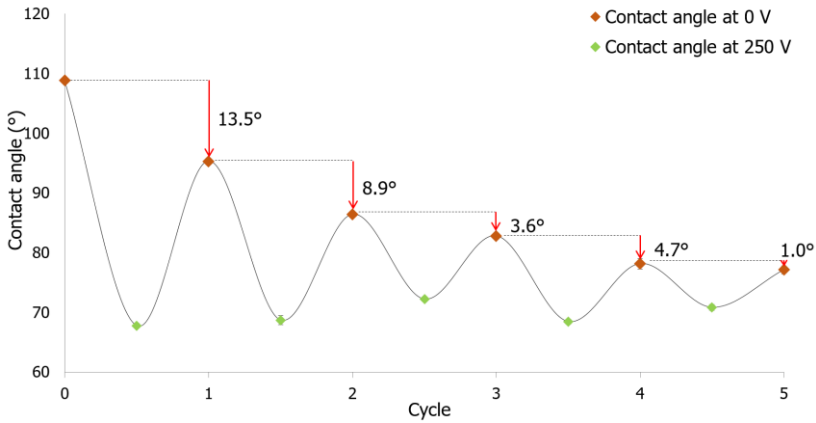

Figure 6: CA evolution of one-layer spray-coated RO-PU during repeated electrowetting cycle

Droplet transportation

The three types of dielectric surfaces that have shown reversibility and good electrowetting efficiency were selected for EWOD plate's fabrication: one-layer spray-coated RO-CC, one-layer spray-coated RO-PU, and two-layer BF. Two EWOD plates were fabricated for each type. The maximum voltage for the droplet actuation is limited to 225 V_{RMS}. Both RO-CC and RO-PU were able to instigate droplet movement to the next electrode at 150 V_{RMS}. As summarized in Table 3, the RO-PU plate 2 has the best performance with reliable droplet actuation across eight electrodes in one of the three electrode arrays at 180 V_{RMS}; both of the RO-PU plates were capable of droplet transportation. One of the RO-CC plates transported droplet across four electrodes at 180 V_{RMS}; the other plate was not functional. Both BF plates were unable to demonstrate any droplet movement. It is believed that the non-functioning BF plates including the non-functioning regions in RO-PU and RO-CC plates could be due to non-uniformity of the dielectric thickness where some areas are thicker than the others, thus requiring a higher voltage of more than 225 V_{RMS} to actuate the droplet. By actuating droplet at 165 V_{RMS} – 180 V_{RMS}, the RO-PU and RO-CC plates have performed comparably well to previously reported devices. Low-cost device which employed Saran™ wrap as dielectric layer operated at 400 - 500 V_{RMS} [15] while another [16] using parafilm required 300 V_{RMS} operating voltage.

Table 3: Droplet transportation performance of EWOD plates with difference types of dielectric layer

Dielectric material	Voltage to instigate droplet movement to the next electrode	Lowest voltage requirement to actuate across three or more electrodes
BF (2-layer)	-	Both plates not functional
RO-CC (1-layer spray-coated)	150 V_{RMS}	Plate 1: not functional Plate 2: 4 electrodes at 180 V_{RMS}
RO-PU (1-layer spray-coated)	150 V_{RMS}	Plate 1: 3 electrodes at 165 V_{RMS} Plate 2: 8 electrodes at 180 V_{RMS}

Conclusions

Polyurethane coatings were investigated for their feasibility as low-cost dielectric in DMF devices by evaluating the electrowetting reversibility of these materials. It has been found that the reversibility of the three selected dielectric PU materials is highly dependent on the thickness of the layer which in turn depends on the method used to deposit the materials. An adequate thickness of the dielectric layer is required to avoid pinholes which cause electrolysis of the droplet when voltage is applied.

The dielectric samples that demonstrated good CA reversibility after voltage application were investigated further to prove their ability to transport droplets across electrodes in an EWOD device. All three materials have shown potential to be used as dielectric component in EWOD, albeit further improvement is needed in terms of the deposition technique. The RO-PU product produced the most promising results by transporting droplet dependably at 180 V_{RMS}. The findings suggest that the key to the successful integration of commercial materials into DMF technology is a deposition method that can produce a layer without pinholes and with uniform thickness reliably across the substrate. Equipment such as an automated spray gun system can help to reduce human error as the amount of substance can be applied consistently whereas manual techniques rely heavily on the operator's skills to produce good surfaces. Spin coating is another deposition method that can be used for these materials but multiple layers are required to overcome the aforementioned failure.

This study proposes commercial PU materials as an approach to address the challenge of high cost in DMF device fabrication. Apart from being low cost, these materials also required simple deposition methods. The evaluated

PU products have shown high potential as the alternative to conventional materials by exhibiting CA reversibility and capability to transport droplets. Hopefully, the findings will contribute towards the realisation of an affordable and robust future DMF device for diagnostic and bio-detection applications.

Contributions of Authors

The authors confirm the equal contribution in each part of this work. All authors reviewed and approved the final version of this work.

Funding

The authors gratefully acknowledge Dato' Azmil Khalid for the funding for this project through PhD Student Scholarship in Engineering.

Conflict of Interests

All authors declare that they have no conflicts of interest

References

[1] Y. Zhang and Y. Liu, "Advances in integrated digital microfluidic platforms for point-of-care diagnosis: a review," *Sensors & Diagnostics*, vol. 1, pp. 648-672, 2022.

[2] B. J. Coelho *et al.*, "Digital Microfluidics for Amplification Monitoring of Cancer Biomarkers," *Materials Proceedings*, vol. 8, no. 1, pp. 103, 2022.

[3] A. B. Alias, H.-Y. Huang, and D.-J. Yao, "A review on microfluidics: An aid to assisted reproductive technology," *Molecules*, vol. 26, no. 14, pp. 4354, 2021.

[4] J. Li, "Current commercialization status of electrowetting-on-dielectric (EWOD) digital microfluidics," *Lab on a Chip*, vol. 20, no. 10, pp. 1705–1712, 2020.

[5] K. Leirs *et al.*, "Bridging the Gap between Digital Assays and Point-of-Care Testing: Automated, Low Cost, and Ultrasensitive Detection of Thyroid Stimulating Hormone," *Analytical Chemistry*, vol. 94, no. 25, pp. 8919-8927, 2022.

[6] L. Malic, D. Brassard, T. Veres, and M. Tabrizian, "Integration and detection of biochemical assays in digital microfluidic LOC devices," *Lab on a Chip*, vol. 10, no. 4, pp. 418–431, 2010.
[7] M. G. Pollack, R. B. Fair, and A. D. Shenderov, "Electrowetting-based actuation of liquid droplets for microfluidic applications," *Applied Physics Letter*, vol. 77, no. 11, pp. 1725–1726, 2000.
[8] H. Liu, S. Dharmatilleke, D. K. Maurya, and A. A. O. Tay, "Dielectric materials for electrowetting-on-dielectric actuation," *Microsystem Technologies*, vol. 16, no. 3, pp. 449, 2010.
[9] F. Mugele and J. Heikenfeld, Electrowetting: Fundamental Principles and Practical Applications, John Wiley & Sons, 2018.
[10] V. Soum *et al.*, "Affordable fabrication of conductive electrodes and dielectric films for a paper-based digital microfluidic chip," *Micromachines*, vol. 10, no. 2, pp. 109, 2019.
[11] V. Narasimhan and S.-Y. Park, "An ion gel as a low-cost, spin-coatable, high-capacitance dielectric for electrowetting-on-dielectric (EWOD)," *Langmuir*, vol. 31, no. 30, pp. 8512–8518, 2015.
[12] J. Chang, D. Y. Choi, S. Han, and J. J. Pak, "Driving characteristics of the electrowetting-on-dielectric device using atomic-layer-deposited aluminum oxide as the dielectric," *Microfluids and Nanofluidics*, vol. 8, no. 2, pp. 269–273, 2010.
[13] Y. Li *et al.*, "Anodic Ta 2 O 5 for CMOS compatible low voltage electrowetting-on-dielectric device fabrication," *Solid-State Electronics*, vol. 52, no. 9, pp. 1382–1387, 2008.
[14] Y.-Y. Lin, R. D. Evans, E. Welch, B.-N. Hsu, A. C. Madison, and R. B. Fair, "Low voltage electrowetting-on-dielectric platform using multi-layer insulators," *Sensors and Actuators B: Chemical*, vol. 150, no. 1, pp. 465–470, 2010.
[15] M. Abdelgawad and A. R. Wheeler, "Low-cost, rapid-prototyping of digital microfluidics devices," *Microfluidics and Nanofluidics*, vol. 4, no. 4, pp. 349, 2008.
[16] M. Yafia, S. Shukla, and H. Najjaran, "Fabrication of digital microfluidic devices on flexible paper-based and rigid substrates via screen printing," *Journal of Micromechanics and Microengineering*, vol. 25, no. 5, pp. 57001, 2015.
[17] M. Jönsson-Niedziółka *et al.*, "EWOD driven cleaning of bioparticles on hydrophobic and superhydrophobic surfaces," *Lab on a Chip*, vol. 11, no. 3, pp. 490–496, 2011.
[18] S.-K. Fan, H. Yang, and W. Hsu, "Droplet-on-a-wristband: Chip-to-chip digital microfluidic interfaces between replaceable and flexible electrowetting modules," *Lab on aChip*, vol. 11, no. 2, pp. 343–347, 2011.
[19] M. Abdelgawad, S. L. S. Freire, H. Yang, and A. R. Wheeler, "All-terrain droplet actuation," *Lab on a Chip*, vol. 8, no. 5, pp. 672–677, 2008.

[20] C. Karuwan *et al.*, "Electrochemical detection on electrowetting-on-dielectric digital microfluidic chip," *Talanta*, vol. 84, no. 5, pp. 1384–1389, 2011.

[21] P. G. Yedewar, S. M. Wadhai, Y. B. Sawane, and A. G. Banpurkar, "Polymethyl methacrylate (PMMA)/fluoropolymer bilayer: a promising dielectric for electrowetting applications," *Journal of Materials Science*, vol. 57, no. 19, pp. 9018–9027, 2022.

[22] C. Dixon, A. H. C. Ng, R. Fobel, M. B. Miltenburg, and A. R. Wheeler, "An inkjet printed, roll-coated digital microfluidic device for inexpensive, miniaturized diagnostic assays," *Lab on a Chip*, vol. 16, no. 23, pp. 4560–4568, 2016.

[23] K. Yamamoto, S. Takagi, Y. Ichikawa, and M. Motosuke, "Electrowetting-on-liquid-dielectric (EWOLD) enables droplet manipulation with a few volts," *arXiv Prepr. arXiv2201.09496*, 2022.

[24] E. N. A. Latip *et al.*, "Protein droplet actuation on superhydrophobic surfaces: A new approach toward anti-biofouling electrowetting systems," *RSC Advances*, vol. 7, no. 78, pp. 49633-49648, 2017.

[25] E. N. A. Latip, "Development of a digital microfluidic toolkit: alternative fabrication technologies for chemical and biological assay platforms." University of Hertfordshire, 2020.

[26] F. Saeki, J. Baum, H. Moon, J.-Y. Yoon, C. J. Kim, and R. L. Garrell, "Electrowetting on dielectrics (EWOD): reducing voltage requirements for microfluidics," *Polymer Materials Science and Engineering*, vol. 85, pp. 12–13, 2001.

[27] H. Moon, S. K. Cho, R. L. Garrell, and C.-J. "CJ" Kim, "Low voltage electrowetting-on-dielectric," *Journal of Applied Physics*, vol. 92, no. 7, pp. 4080–4087, 2002.